

Robustness of Energy Landscape Controllers for Spin Rings under Coherent Excitation Transport

Sean P. O'Neil,^{*,1} Frank C. Langbein,^{*,2} Edmond Jonckheere,^{*,1} and S. Shermer^{*,3}

¹Department of Electrical and Computer Engineering, University of Southern California, Los Angeles, CA 90089

²School of Computer Science and Informatics, Cardiff University, Cardiff CF24 4AG, UK

³Faculty of Science and Engineering, Physics, Singleton Park, Swansea, SA2 8PP, UK

Article

Keywords:

spin networks, coherent excitation transfer, energy landscape control, robust control

*Author for correspondence. Email: seanonei@usc.edu; frank@langbein.org; jonckhee@usc.edu; s.m.shermer@gmail.com

Abstract

The design and analysis of controllers to regulate excitation transport in quantum spin rings presents challenges in the application of classical feedback control techniques to synthesize effective control, and generates results in contradiction to the expectations of classical control theory. In this paper, we examine the robustness of controllers designed to optimize the fidelity of an excitation transfer to uncertainty in system and control parameters. We use the logarithmic sensitivity of the fidelity error as the measure of robustness, drawing on the classical control analog of the sensitivity of the tracking error. In our analysis we demonstrate that quantum systems optimized for coherent transport demonstrate significantly different correlation between error and the log-sensitivity depending on whether the controller is optimized for readout at an exact time T or over a time-window $T \pm \Delta T$.

1. Introduction

Excitation transfer in the single-excitation subspace of a ring of spin $\frac{1}{2}$ particles coupled via XXZ coupling forms a simple model for information transfer in a spintronic router (Sophie G Schirmer, Edmond Jonckheere, and F. G. Langbein 2015; Sophie G. Schirmer, E. A. Jonckheere, and F. C. Langbein 2018). Design of controls for such systems is non-trivial. Most fundamentally, measurement of the quantum state in the usual feedback control paradigm would alter the dynamics of the quantum system in a probabilistic manner (Wiseman and Milburn 2009). Additionally, the coherent dynamics of a quantum system result in trajectories that evolve unitarily with all eigenvalues on the imaginary axis and are thus not asymptotically stable (Weidner et al. 2022). Taken together, this precludes the application of common linear control techniques such as full-state feedback or pole placement.

To obviate such roadblocks to development of classically-inspired controls, the work this analysis is based on appeals to the solution of a non-convex optimization problem to generate optimal, time-independent controllers (Sophie G Schirmer, Edmond Jonckheere, and F. G. Langbein 2015). The controllers considered are designed to alter the energy landscape of a quantum ring via static bias fields to facilitate the transfer of a single excitation from an initial spin $|IN\rangle$ to a target spin $|OUT\rangle$ with maximum fidelity at a given time T or over a (readout) time window $T \pm \Delta T$ under unitary dynamics.

While design of realizable controllers is one challenge, ensuring these controllers' robustness to external perturbations or parameter uncertainty is necessary to fully harness any benefits of emerging quantum technology (Shermer 2023; Glaser et al. 2015). Various control designs for specific applications claiming robustness have been proposed (Kosut, Bhole, and Rabitz 2022; Ram et al. 2022; Zhang et al. 2022; Valahu et al. 2022; Koswara, Bhutoria, and Chakrabarti 2021; Dridi, Liu, and Guérin 2020; Wu et al. 2019; Güngördü and Kestner 2019; Shapira et al. 2018; Deng, Barnes, and Economou 2017; Daems et al. 2013) but a comprehensive framework for robust control for quantum systems is lacking. Again, the unique characteristics of quantum systems present challenges in analyzing the robustness of control schemes. The marginal stability of open quantum systems precludes the use of common small gain theorem-based techniques such as structured singular value analysis (Zhou and Doyle 1998). Also, in contrast to classical control problems based on asymptotic response, excitation transfer is an inherently time-domain problem requiring a time-domain view of robustness that differs from classical frequency domain methods (Sontag 1998; S. O'Neil et al. 2022).

In this analysis paper, we explore the design of time-optimal controllers published as Frank Langbein, Sean O’Neil, and Shermer (2022) and analyze their robustness through a time-domain logarithmic sensitivity measure. The correlation between error and log-sensitivity of the controllers in this data set was first explored in E. Jonckheere, S. Schirmer, and F. Langbein (2018) and identified the non-conventional trend of controllers optimized for time-windowed readout. In this paper we expand the analysis to include controllers optimized for instant-time read-out as well to better understand the robustness of the entire range of possible controllers, leading to the identification of factors that yield greater robustness. The analysis shows that controllers optimized for exact-time excitation transfer exhibit behavior in the trade-off between robustness and performance expected of a classical feedback control system. In contrast, those controllers optimized to maximize transfer over a time-window display trends between performance and robustness in contradiction to expectations. Further, in this analysis we apply a modified log-sensitivity calculation that accounts for averaging over the read-out window, a factor not accounted for in previous work.

The remainder of this paper is organized in the following manner. In Section 2.1 we present the mathematical model for a spin-1/2 ring, derive the evolution for excitation transfer, and define the performance measure of fidelity. In Section 2.2 we present the optimization scheme for maximizing the fidelity, and in Section 2.3 we define the time-domain log-sensitivity used to gauge the robustness of the controllers. In Section 3 we present the hypothesis testing used to judge the conventional versus non-conventional relationship between performance (measured as the fidelity) and robustness (measured as the size of the log-sensitivity). We then present the results of the hypothesis test and identify additional robustness features not highlighted by the statistical analysis. We then conclude in Section 4.

2. Methods

2.1 System Description, Dynamics, and Fidelity

Consider a set of N interacting spin- $\frac{1}{2}$ particles with only one spin in an excited state and the remainder in the ground state. In this single-excitation sub-space, the network can be represented by a $N \times N$ total Hamiltonian H_0 with

$$H_0 = \hbar \sum_{m \neq n} J_{mn} (X_m X_n + Y_m Y_n + \kappa Z_m Z_n). \quad (1)$$

Here, the J_{mn} are the couplings between spin n and m , measured in units of frequency, and \hbar is the reduced Planck constant. In general $J_{mn} = J_{nm}$, and for a ring topology with nearest-neighbor coupling, J_{mn} is only non-zero for $n = m \pm 1$ and $J_{1N} = J_{N1}$. In particular, we consider the case of uniform coupling so that $J_{mn} = J_{nm} = J$ for all m, n . The terms X_n, Y_n, Z_n are the Pauli spin operators acting on spin n . These are N -fold tensor products whose n th factor is one of the Pauli matrices

$$X = \begin{pmatrix} 0 & 1 \\ 1 & 0 \end{pmatrix}, \quad Y = \begin{pmatrix} 0 & -j \\ j & 0 \end{pmatrix}, \quad Z = \begin{pmatrix} 1 & 0 \\ 0 & -1 \end{pmatrix}$$

and all other factors are the 2×2 identity matrix I . The parameter κ distinguishes different coupling types such as XX-coupling ($\kappa = 0$) or Heisenberg coupling ($\kappa = 1$); specifically we consider XX-coupling. We justify restricting our attention to XX-coupling based on the control scheme introduced in Section 2.2. In short, this scheme is based on spin-addressable bias fields modeled as diagonal elements of the Hamiltonian. As Heisenberg coupling introduces purely diagonal coupling terms into the Hamiltonian, they can be absorbed into the diagonal control elements so that the system model is equivalent to a strictly XX-coupled system.

We represent the state of the system by a wavevector $|\psi\rangle \in \mathbb{C}^N$ whose n th entry represents the state of spin n . Specifically, if spin n is measured to be in the excited state with absolute certainty, the n th entry of $|\psi\rangle$ has magnitude 1. Conversely, if the spin has zero probability of being excited the entry is 0, indicating the spin is in the ground state. A value of $0 < |\psi_n| < 1$ indicates the n th spin has a non-zero probability to be excited. The probability that the state $|\psi\rangle$ is the same as the state $|\psi_0\rangle$ is given by $|\langle \psi_0 | \psi \rangle|^2$, and $|\langle \psi | \psi \rangle|^2 = 1$. Associating the N state vectors $\{|\psi_n\rangle\}$ which indicate a single excitation on spin n with the natural basis vectors of \mathbb{C}^N provides a convenient basis for describing the system dynamics.

In this basis, considering only XX-coupling and ring topology, the Hamiltonian of (1) takes the explicit form

$$H_0 = \hbar \begin{pmatrix} 0 & J_{1,2} & 0 & \dots & 0 & J_{1,N} \\ J_{1,2} & 0 & J_{2,3} & & 0 & 0 \\ 0 & J_{2,3} & 0 & & 0 & 0 \\ \vdots & & & \ddots & & \vdots \\ 0 & 0 & 0 & & 0 & J_{N-1,N} \\ J_{1,N} & 0 & 0 & \dots & J_{N-1,N} & 0 \end{pmatrix}. \quad (2)$$

The dynamical evolution of this system is governed by the time-dependent Schrödinger equation:

$$\frac{d}{dt} |\psi(t)\rangle = -\frac{i}{\hbar} H_0 |\psi(t)\rangle, \quad |\psi(0)\rangle = |\psi_0\rangle. \quad (3)$$

Assuming a system of units where $\hbar = 1$, the solution to (3) is

$$|\psi(t)\rangle = e^{-itH_0} |\psi_0\rangle = U(t) |\psi_0\rangle. \quad (4)$$

Noting that H_0 is Hermitian with real eigenvalues, we can immediately see that the eigenvalues of the open-loop system are purely imaginary, and so the system is not stable, but only marginally stable (Chen 2013). In simplest terms, this means there is no asymptotic steady state of the system, as evident from the eigenvalues of the form $-i\lambda$. This presents two conflicting issues in the control of closed quantum systems. On the one hand, the unitary evolution of the system is desirable in retaining the coherence or phase of the system that ultimately permits the benefits of quantum technology. On the other hand, the techniques of classical control theory (pole-placement, full-state feedback, etc.) require synthesis of *stabilizing* controllers (Dorf and Bishop 2000). While this is prudent from a classical point of view in that stabilizing

controllers preclude the possibility of an unbounded response, applied to a quantum system, this would result in convergence to a classical steady state, resulting in the loss of coherence. We thus see one case for the development of control techniques outside the scope of established classical feedback control.

We now consider the problem of transferring the single excitation of the system from a given input spin $|IN\rangle = |\psi_0\rangle$ to a specific output spin $|OUT\rangle$. At a given time T the probability that $|\psi(t)\rangle = |OUT\rangle$ is given by the overlap squared of the current state with the target state or

$$\mathcal{F}(T) = |\langle OUT | \psi(T) \rangle|^2 = |\langle OUT | U(T) | IN \rangle|^2 \quad (5)$$

where $\mathcal{F}(T)$ is the fidelity of the transfer at time T . Extending this concept to a time-window of $\pm\Delta T$ about the time T , we define the time-averaged fidelity as

$$\mathcal{F}(T \pm \Delta T) = \frac{1}{2\Delta T} \int_{T-\Delta T}^{T+\Delta T} |\langle OUT | U(t) | IN \rangle|^2 dt. \quad (6)$$

Finally, noting that the upper bound on both $\mathcal{F}(T)$ and $\mathcal{F}(T \pm \Delta T)$ is unity, we define the fidelity error in analogy to the tracking error as

$$\begin{aligned} e(T) &= 1 - \mathcal{F}(T) \\ e_{\Delta}(T) &= 1 - \mathcal{F}(T \pm \Delta T). \end{aligned} \quad (7)$$

2.2 Design Goals and Optimization Scheme

Consider the design goal of maximizing the fidelity for the instant time case (5) or the time-averaged case (6). To obviate the issues of backaction involved in measurement-based feedback control we introduce control via static bias-fields that ideally address a single spin to alter the energy landscape of the system. In terms of the Hamiltonian (2), these control fields take the form

$$D = \sum_{n=1}^N D_n = d_n |n\rangle \langle n|. \quad (8)$$

Here, $D_n \in \mathbb{R}^{N \times N}$ and consists of all zeros, save for the n th diagonal element which assumes the scalar value d_n of the field addressing spin n . This augments the natural Hamiltonian so that $H_D = H_0 + D$. The state transition matrix is thus modified as $U_D(t) = e^{-it(H_0+D)}$, and likewise the expressions for the fidelity in (5) and (6).

Maximization of the fidelity at a specific time T or over a window $T \pm \Delta T$ then becomes a non-convex optimization problem of the form

$$\min_{\{D_n, T\} \in \mathbb{X}} \left[1 - |\langle OUT | e^{-iT(H_0 + \sum_n D_n)} | IN \rangle|^2 \right] \quad (9)$$

or

$$\min_{\{D_n, T\} \in \mathbb{X}} \left[1 - \frac{1}{2\Delta T} \int_{T-\Delta T}^{T+\Delta T} |\langle OUT | e^{-it(H_0 + \sum_n D_n)} | IN \rangle|^2 dt \right]. \quad (10)$$

Here, \mathbb{X} defines the set of admissible controllers D_n and readout times T defined by the optimization constraints.

The controllers used in this study were developed using the MATLAB's *fminunc* solver with BFGS quasi-Newton algorithm. The optimization was performed with a bias toward producing high fidelity controllers by choosing start times corresponding to high-fidelity peaks in the transfer of an equivalent chain between $|IN\rangle$ and $|OUT\rangle$ as initial values for the time variable in the optimization. Further, we placed symmetry conditions on the possible values of D_n . Specifically, the $D_n = d_n |n\rangle \langle n|$ were constrained so that $d_{IN} = d_{OUT}$ and $d_{IN+k} = d_{OUT-k}$ for $k \in \{1 \dots \lceil (OUT-IN)/2 \rceil\}$. See Sophie G Schirmer, Edmond Jonckheere, and F. G. Langbein (2015) for a more detailed exposition of the optimization and constraints.

2.3 Robustness Measure - Log-Sensitivity

Given a system model and controls to maximize the fidelity, we now consider the issue of robustness of the control scheme to uncertainty in the system parameters or control fields. We denote an uncertain parameter (coupling coefficient or bias field) as $\xi_{\mu} \in \mathbb{R}$ such that

$$\xi_{\mu} = \begin{cases} d_{\mu} + \delta_{\mu}, & 1 \leq \mu \leq N \\ J_{(\mu-N),(\mu-N+1)} + \delta_{\mu}, & N+1 \leq \mu \leq 2N-1 \\ J_{1,N} + \delta_{\mu}, & \mu = 2N \end{cases} \quad (11)$$

so that $\mu \in \{1, \dots, N\}$ correspond to perturbations to the control and $\mu \in \{N+1, \dots, 2N\}$ corresponds to perturbations to the Hamiltonian. Here $\delta_{\mu} \in \mathbb{R}$ represents the deviation from the nominal value in compatible physical units with ξ_{μ} .

These uncertainties enter the Hamiltonian through structure matrices $S_{\mu} \in \mathbb{R}^{N \times N}$. The uncertain Hamiltonian now becomes $\tilde{H}_D = H_0 + D + \sum_{\mu} \delta_{\mu} S_{\mu}$. Specifically we define:

$$S_{\mu} = \begin{cases} | \mu \rangle \langle \mu |, & 1 \leq \mu \leq N \\ | \mu - N \rangle \langle \mu - N + 1 | + | \mu - N + 1 \rangle \langle \mu - N |, & N+1 \leq \mu \leq 2N-1 \\ | 1 \rangle \langle N | + | N \rangle \langle 1 |, & \mu = 2N \end{cases} \quad (12)$$

Consequently, we have the uncertain state-transition matrix as $\tilde{U}(t) = e^{-it(H_0 + D + \sum_{\mu} \delta_{\mu} S_{\mu})}$. Now considering a single uncertain parameter in the Hamiltonian, we can look at the differential sensitivity of the state transition matrix to that parameter as

$$\begin{aligned} \frac{\partial \tilde{U}(T)}{\partial \xi_{\mu}} &= \lim_{\Delta \xi_{\mu} \rightarrow 0} \frac{e^{-it\tilde{H}_D(\xi_{\mu})} - e^{-it\tilde{H}_D(\xi_{\mu 0})}}{\Delta \xi_{\mu}} \\ \frac{\partial \tilde{U}(T)}{\partial \delta_{\mu}} &= \lim_{\delta_{\mu} \rightarrow 0} \frac{e^{-it(H_0 + D + \delta_{\mu} S_{\mu})} - e^{-it(H_0 + D)}}{\delta_{\mu}} \end{aligned} \quad (13)$$

where ξ_{μ} is defined as in (11) with nominal value given by $\xi_{\mu 0}$ when $\delta_{\mu} = 0$.

Here we note the differential sensitivity of (13), in both equivalent forms, is valuable in it's own right as a measure the effect of parameter uncertainty on $e(T)$. However, this pure differential sensitivity carries an intrinsic scaling by the physical units of the parameter in the denominator of the limit.

While this permits a useful comparison in sensitivity for the same type of uncertainty, it does not provide an unbiased measure for comparing robustness between different uncertainty categories. For this reason, we seek a *dimensionless* measure of robustness in the logarithmic sensitivity, requiring renormalization of the terms in (13) by $\xi_{\mu}/\tilde{U}(T)|_{\xi_{\mu}=\xi_{\mu 0}} = U^{\dagger}(T)\xi_{\mu 0}$ or $\delta_{\mu}/\tilde{U}(T)|_{\xi_{\mu}=\xi_{\mu 0}} = U^{\dagger}(T)\delta_{\mu 0}$. Even though $\partial/\partial\xi_{\mu} = \partial/\partial\delta_{\mu}$, these two normalization factors result in different log-sensitivities. This is obvious by noting that $U^{\dagger}(T)\xi_{\mu 0} \neq 0$ while $U^{\dagger}(T)\delta_{\mu 0} = 0$. Finally, observe that if the uncertain parameter has a nominal value of zero, the log-sensitivity formulation above requires modification to consider only deviations from the nominal value while producing a non-trivial measure of sensitivity.

Noting that the performance measure $\mathcal{F}(\cdot)$ is time-based, we assess the robustness of the control scheme by determining the differential effect of uncertainty on the fidelity error $e(T)$ or $e_{\Delta}(T)$ as defined in (7) (equally the fidelity) in both the instant read-out and windowed readout case through the logarithmic sensitivity

$$s(\xi_{\mu 0}, T) = \left. \frac{\partial e(T)}{\partial \xi_{\mu}} \frac{\xi_{\mu}}{e(T)} \right|_{\xi_{\mu 0}} \quad (14)$$

for instantaneous readout and

$$s_{\Delta}(\xi_{\mu 0}, T) = \left. \frac{\partial e_{\Delta}(T)}{\partial \xi_{\mu}} \frac{\xi_{\mu}}{e_{\Delta}(T)} \right|_{\xi_{\mu 0}} \quad (15)$$

We see that (14) is then the differential sensitivity of the fidelity error normalized by the ratio of the nominal parameter value and value of the fidelity error.

Consider a decomposition of $e^{-it(H_0+D)} = \sum_{n=1}^N \Pi_n e^{-it\lambda_n}$, and let $\omega_{mn} = \lambda_m - \lambda_n$. Here Π_n are the projectors onto the orthogonal subspaces of the controlled Hamiltonian H_D . Specifically, from the spectral decomposition of $H_D = V\Lambda V^{\dagger}$, λ_n is the n th diagonal entry of Λ and Π_n is the dyadic product of the n th column of V with itself or $\Pi_n = V_n V_n^{\dagger}$. Then for $e(T) = 1 - \mathcal{F}(T)$ and we have from Sophie G. Schirmer, E. A. Jonckheere, and F. C. Langbein (2018)

$$\begin{aligned} \frac{\partial e(T)}{\partial \delta_{\mu}} &= 2T \sum_{m,n} \langle \text{OUT} | \Pi_m S_{\mu} \Pi_n | \text{IN} \rangle \text{sinc} \left(\frac{1}{2} T (\omega_{mn}) \right) \\ &\times \sum_p \langle \text{IN} | \Pi_p | \text{OUT} \rangle \sin \left(\frac{1}{2} T (\omega_{mp} + \omega_{np}) \right) \end{aligned} \quad (16)$$

where $\text{sinc}(x) = \frac{\sin(x)}{x}$. For $e_{\Delta}(T) = 1 - \mathcal{F}(T \pm \Delta T)$ we have a more complicated expression

$$\frac{\partial e_{\Delta}(T)}{\partial \delta_{\mu}} = \sum_{\lambda_m = \lambda_n \neq \lambda_p} A(T, \Delta, \lambda_m, \lambda_p) + \sum_{\lambda_m \neq \lambda_n} B(T, \Delta, \lambda_m, \lambda_n, \lambda_p). \quad (17)$$

Note that for $\lambda_n = \lambda_m = \lambda_p$ there is no contribution to the sum.

Specifically we have

$$\begin{aligned} A(T, \Delta, \lambda_m, \lambda_p) &= \frac{1}{\Delta} \langle \text{OUT} | \Pi_p | \text{IN} \rangle \langle \text{IN} | \Pi_m S_{\mu} \Pi_m | \text{OUT} \rangle \times \\ &\left\{ \frac{2}{\omega_{mp}} \left[\left(T + \frac{\Delta}{2} \right) \cos[\omega_{mp}(T + \frac{\Delta}{2})] - \left(T - \frac{\Delta}{2} \right) \cos[\omega_{mp}(T - \frac{\Delta}{2})] \right] \right. \\ &\left. - \frac{2}{\omega_{mp}^2} \left(\sin[\omega_{mp}(T + \frac{\Delta}{2})] - \sin[\omega_{mp}(T - \frac{\Delta}{2})] \right) \right\} \end{aligned} \quad (18)$$

and

$$\begin{aligned} B(T, \Delta, \lambda_m, \lambda_n, \lambda_p) &= \\ &\frac{1}{\Delta} \frac{2}{\omega_{mn}} \langle \text{OUT} | \Pi_p | \text{IN} \rangle \langle \text{IN} | \Pi_m S_{\mu} \Pi_n | \text{OUT} \rangle \\ &\times \left(\left(T + \frac{\Delta}{2} \right) \text{sinc} \left[\omega_{mp}(T + \frac{\Delta}{2}) \right] - \left(T - \frac{\Delta}{2} \right) \text{sinc} \left[\omega_{mp}(T - \frac{\Delta}{2}) \right] \right) \\ &- \left(T + \frac{\Delta}{2} \right) \text{sinc} \left[(\omega_{np})(T + \frac{\Delta}{2}) \right] + \left(T - \frac{\Delta}{2} \right) \text{sinc} \left[(\omega_{np})(T - \frac{\Delta}{2}) \right] \end{aligned} \quad (19)$$

We use differential sensitivity established by (16) and (17) normalized by the ratio $\frac{\xi_{\mu 0}}{e(T)}$ or $\frac{\xi_{\mu 0}}{e_{\Delta}(T)}$ so as to get a nontrivial, i.e., non-vanishing, log-sensitivity as measure of robustness.

3. Analysis

Our analysis of the controllers produced by the optimization in Section 2.2 consists of two parts: (1) statistical hypothesis testing of the relationship between performance, as measured by the size of the fidelity error, and robustness, gauged by the size of the log-sensitivity and (2) identification of areas that require more exploration to explain the observed robustness properties.

3.1 Classical control considerations

As discussed in previous work E. Jonckheere, S. Schirmer, and F. Langbein (2018), O'Neil et al. (2017), and S. Schirmer et al. (2018) the classical limitations on the size of allowable perturbations and level of desired performance is limited in the field of classical feedback control though the identity $\hat{S}(s) + \hat{T}(s) = I$. Here $\hat{S}(s) = (I + \hat{L}(s))^{-1}$ where $\hat{L}(s)$ is the loop transfer function matrix of a single-degree of freedom feedback system with negative unity feedback (Chen 2013; Dorf and Bishop 2000). Defining the Laplace transform of the reference input at $\hat{r}(s)$ and that of the measured output as $\hat{y}(s)$ so that the error between desired output and measured output is $\hat{e}(s) = \hat{r}(s) - \hat{y}(s)$, the sensitivity function represents the frequency-dependent mapping from the reference to the error or $\hat{e}(s) = \hat{S}(s)\hat{r}(s)$. The mapping from the system input to the output is measured through the complementary sensitivity function so that $\hat{y}(s) = \hat{T}(s)\hat{r}(s)$ where $\hat{T}(s) = (I + \hat{L}(s))^{-1} \hat{L}(s)$. Considering an uncertain plant and/or controller with uncertain parameter ξ , we have that the differential sensitivity of $\hat{L}(s)$ to changes in ξ is given by:

$$\hat{S}(s)^{-1} \frac{d\hat{S}(s)}{d\xi} = -\frac{d\hat{L}(s)}{d\xi} \hat{L}(s)^{-1} \hat{T}(s). \quad (20)$$

Applying the normalization of (13) and evaluating the expression at the nominal value of ξ_{μ} we can recast the above as

$$\xi_{\mu 0} \hat{S}(s)^{-1} \left. \frac{d\hat{S}(s)}{d\xi} \right|_{\xi_{\mu}=\xi_{\mu 0}} = -\xi_{\mu 0} \left. \frac{d\hat{L}(s)}{d\xi} \hat{L}(s)^{-1} \hat{T}(s) \right|_{\xi_{\mu}=\xi_{\mu 0}}. \quad (21)$$

Or written more compactly in terms of a dimensionless logarithmic relation we have

$$\frac{d \ln \hat{S}(s)}{d \ln \xi} = - \frac{d \ln \hat{L}(s)}{d \ln \xi} \hat{T}(s). \quad (22)$$

We see that (22) implies that acceptable performance (i.e., $\hat{T}(s) \approx I$) limits the controller ability to reduce the open-loop sensitivity $d \ln \hat{L}(s)/d \ln \xi$ to a lower closed-loop sensitivity $d \ln \hat{S}(s)/d \ln \xi$. Conversely, the same equation (22) implies that a small closed-loop log-sensitivity to parameter variation requires lower performance (a smaller gain in $\hat{T}(s)$). From a slightly different perspective, $S + T = I$ quantifies the need to trade-off between good performance ($\hat{S}(s)$ small) and good robustness ($\hat{T}(s)$ small).

The goal now is to quantify how well the static controllers developed for the energy landscape scheme accord with this classical limitation on performance and sensitivity. To do this, we must still establish that $\frac{\partial e}{\partial \xi}$ is proportional to $\frac{\partial \hat{S}}{\partial \xi}$. We first note that the performance index as defined by (5) and (6) is a time-domain specification and not dependent on asymptotic convergence of the measured output with the desired output. We next note that the error as defined by (7) has a non-linear relation with the reference input $|OUT\rangle$. Taken together, this precludes a direct analog with the Laplace-transform relations of (22). However, we use this functional dependence of $e(T)$ and $e_{\Delta}(T)$ with $|OUT\rangle$ to draw a time-domain parallel with $\hat{e}(s) = \hat{S}(s)\hat{r}(s)$. Specifically, for $\|\hat{e}(s)\| \in \mathbb{R}$ and $\hat{r}(s) \in \mathbb{C}^N$, a specific $\hat{S}(s)$ defines a map F

$$F(\hat{S}(s), \cdot) : \mathbb{C}^N \rightarrow \mathbb{R} \\ \hat{r}(s) \mapsto \|\hat{e}(s)\|,$$

where $\hat{S}(s) = (I + \hat{L}(s))^{-1}$ and $F(\hat{S}(s), \hat{r}(s)) = \|\hat{S}(s)\hat{r}(s)\|$. In terms of the time-domain specification, we have that for $\|e(t)\|$ of the time-domain specification, we have that for $\|e(t)\| \in \mathbb{R}$ and $|OUT\rangle \in \mathbb{C}^N$ we can construct an analogous map G

$$G(\tilde{S}(t), \cdot) : \mathbb{C}^N \rightarrow \mathbb{R} \\ |OUT\rangle \mapsto \|e(t)\|$$

defined by $G(\tilde{S}(t), |OUT\rangle) = \tilde{S}(t) = 1 - |\langle OUT | U(t) | IN \rangle|^2$. Given an input $\hat{r}(s)$ or $|OUT\rangle$ that do not depend on the uncertain parameter ξ , we then see that in the frequency domain formulation $\frac{\partial \hat{e}(s)}{\partial \xi} = \left[\frac{\partial F}{\partial \hat{S}} \right] \frac{\partial \hat{S}}{\partial \xi} \propto \frac{\partial \hat{S}(s)}{\partial \xi}$ or the sensitivity of the norm of the error is proportional to the sensitivity of the frequency domain sensitivity function. Extending this to the time domain mapping have also that $\frac{\partial e(t)}{\partial \xi} = \left[\frac{\partial G}{\partial \tilde{S}} \right] \frac{\partial \tilde{S}}{\partial \xi} \propto \frac{\partial \tilde{S}}{\partial \xi}$.

In both cases we have that the error is proportional to the sensitivity of the sensitivity function to parameter variation and rely on the differential log sensitivity of the error $s(\xi_0, T)$ as defined by (14) to evaluate robustness versus the performance index established in (5) and (6).

3.2 Hypothesis Test

We establish the following two-tailed hypothesis test to confirm or refute whether the controllers in this data set conform to the conventional limitations on robustness and performance established above. For brevity in the following section we will describe the hypothesis testing in terms of $e(T)$ versus $s(\xi_{\mu 0}, T)$, but the conditions apply equally to $e_{\Delta}(T)$ and $s_{\Delta}(\xi_{\mu 0}, T)$:

- H_0 - null hypothesis postulating no trend between $s(\xi_{\mu 0}, T)$ and $e(T)$,
- H_{1+} - alternative hypothesis one postulating positive correlation between $s(\xi_0, T)$ and $e(T)$ and indicative of controllers that do not exhibit the conventional limitation on performance and robustness,
- H_{1-} - alternative hypothesis two postulating negative correlation between $s(\xi_0, T)$ and $e(T)$ and indicative of controllers that exhibit the conventional limitation on performance and robustness.

To execute the test we chose two distinct correlation measures: the Kendall τ as a non-parametric test based on rank-ordering of the data (Abdi n.d.) and the Pearson r linear correlation coefficient to test the linear relation between the two metrics on a log-log scale. We chose rings sizes from $N = 3$ to $N = 20$. For all controllers examined, the initial state is taken as $|IN\rangle = |1\rangle$ so that the excitation is initially located at spin-1. For the time-windowed readout controllers (the dt controllers) we tested excitation transfer ranging from localization at the initial spin $|IN\rangle = |OUT\rangle = |1\rangle$ up to $|OUT\rangle = \left| \left[\frac{N}{2} \right] \right\rangle$. For the instant readout case (the t controllers) we consider transfers from $|OUT\rangle = |2\rangle$ through $|OUT\rangle = \left| \left[\frac{N}{2} \right] \right\rangle$. We note that there is nothing unique in the selection of $|1\rangle$ as the initial spin as the ring is rotationally symmetric. Likewise consideration of transfers only up to $\left[\frac{N}{2} \right]$ is justified by the symmetry of the ring as well. This provides a total of 90 test cases for the instantaneous readout controllers and 108 test cases for the time-windowed readout case. Though a complete set of 2000 controllers exists for each possible transfer, we filter controllers that produce a fidelity $\mathcal{F} < 0.9$, and base our analysis on the remaining controllers, maintaining consistency with the analysis in E. Jonckheere, S. Schirmer, and F. Langbein (2018).

To compute the degree of correlation between $e(T)$ and $s(\xi_0, T)$ for each ring and transfer combination, we apply the `corr` function from MATLAB with options 'Kendall' to produce the Kendall τ and 'Pearson' to generate the Pearson r . With the raw Kendall τ and Pearson r we establish the threshold for statistical significance at $\alpha = 0.01$ to reject H_0 in favor of H_{1+} for a positive (rank) correlation coefficient and in favor of H_{1-} for a negative (rank) correlation coefficient. We judge the level of significance for each possible

test case depending on the correlation coefficient used. For the Kendall τ we normalize by the standard deviation so that $Z_\tau = \tau \left(\sqrt{\frac{2(2n+5)}{9n(n-1)}} \right)^{-1}$ where n is the number of samples (controllers) within the test case. We then quantify the statistical significance of the results through their p -values defined as

$$p_\tau = \begin{cases} \Phi(Z_\tau), & \tau < 0 \\ 1 - \Phi(Z_\tau), & \tau > 0 \end{cases} \quad (23)$$

where Φ is the normal cumulative distribution function. To evaluate the statistical significance of the Pearson r , we translate the raw correlation coefficient to a t -statistic through $t_r = r \left(\sqrt{\frac{1-r^2}{n-2}} \right)^{-1}$. We then quantify the statistical significance of the test for a given value of r as

$$p_r = \begin{cases} \mathcal{S}(t_r), & r < 0 \\ 1 - \mathcal{S}(t_r), & r > 0 \end{cases} \quad (24)$$

where \mathcal{S} represents the cumulative Student’s t -distribution.

Finally, though we are generally looking at the trend of $s(\xi_{\mu 0}, T)$ versus $e(T)$, there are a total of $2N$ perturbation directions to examine for each excitation transfer. To streamline the analysis, we focus specifically on three categories of perturbation within each possible transfer and ring:

- Norm over the N controller perturbations—in this case we examine the trend of $e(T)$ versus $\|s(\xi_{\mu 0}, T)\|_C = \sqrt{\sum_{\mu=1}^N |s(\xi_{\mu 0}, T)|^2}$.
- Norm over the N Hamiltonian uncertainties—in this case we examine the trend of $e(T)$ versus $\|s(\xi_{\mu 0}, T)\|_H = \sqrt{\sum_{\mu=N+1}^{2N} |s(\xi_{\mu 0}, T)|^2}$.
- Norm of all $2N$ uncertainties—in this case we examine the trend of $e(T)$ versus $\|s(\xi_{\mu 0}, T)\| = \sqrt{\sum_{\mu=1}^{2N} |s(\xi_{\mu 0}, T)|^2}$.

We present the results in the following section in terms of these uncertainty categories.

3.3 Hypothesis Test Results

The entire spreadsheet depicting the results of hypothesis test is available in the repository Frank Langbein, Shermer, and Sean O’Neil (2023). We present the following summary of significant deductions from the hypothesis test:

3.3.1 Instant Readout Controllers (t Controllers)

The trend between $e(T)$ and each normed measure of $s(\xi_{\mu 0}, T)$, measured by the Kendall τ for rank correlation, is overwhelmingly conventional, showing a negative correlation between error and log-sensitivity, save for the transfer from spin 1 to spin 2 or nearest-neighbor transfer. For nearest-neighbor transfer the hypothesis test rejects H_0 in favor of

H_{1+} for all nearest-neighbor transfers for $N \geq 7$. None of the tests for the nearest-neighbor transfer fail to meet the $\alpha = 0.01$ threshold and are thus considered reliable. Though not the complete list of results, Table 1 provides a snapshot of the hypothesis test for the correlation between $e(T)$ and $\|s(\xi_{\mu 0}, T)\|$ for $N = 3$ to $N = 12$. In detail:

- For the $e(T)$ versus $\|s(\xi_{\mu 0}, T)\|$ correlation, five of the 90 tests fail to achieve a significance level of $\alpha = 0.01$ and are excluded. Of the remaining tests, all display a conventional negative trend, save for the nearest-neighbor transfers noted above.
- Of the 90 tests for $e(T)$ versus $\|s(\xi_{\mu 0}, T)\|_C$, all but nine display a conventional trend with a confidence of at least 99%. Of these nine tests, all fall into the category of nearest-neighbor transfer, seven display a p -value greater than α and are discarded, and the other two display a non-conventional positive trend.
- The tests for $e(T)$ versus $\|s(\xi_{\mu 0}, T)\|_H$ follows the same pattern as that of $\|s(\xi_{\mu 0}, T)\|$ with nearest-neighbor transfers displaying a non-conventional trend with high confidence, except for $N < 6$ cases. Of the remaining tests, all show a conventional trend except for nine cases that fail to meet the required confidence level,

As a check on consistency, we compare the hypothesis test results based on the rank-correlation of the Kendall τ with the results based on the linear correlation coefficient of Pearson’s r . Though not identical, the hypothesis tests based on each measure show strong agreement as summarized below.

- For the $\|s(\xi_{\mu 0}, T)\|$ tests, the hypothesis tests provide identical results in terms of acceptance or rejection of H_0 with two exceptions, neither of which affect the non-conventional trend for nearest-neighbor transfer. For the Pearson r -based test, the $N = 6, 1 \rightarrow 2$ test does not display the confidence to reject the null-hypothesis as in the Kendall τ -based test. Conversely, while the $N = 12$ and $1 \rightarrow 6$ transfer is unable to reject H_0 for the Kendall τ test, the Pearson r test does reject the null hypothesis in favor of H_{0-} .
- The comparison for $\|s(\xi_{\mu 0}, T)\|_C$ shows strong consistency, agreeing in rejection of H_0 in favor of H_{1-} for all transfers except for $N \geq 11$ nearest-neighbor transfers with one exception—the Pearson r test is inconclusive for the $N = 10$ nearest-neighbor transfer. Of the remaining nine nearest-neighbor tests, the Pearson r test provides higher confidence, with seven of the nine rejecting H_0 in favor of H_{1+} with high confidence.
- The Pearson r -based hypothesis test for $e(T)$ versus $\|s(\xi_{\mu 0}, T)\|_H$ agrees with the Kendall τ in rejection of H_0 for all nearest-neighbor transfer for $N \geq 6$ but displays ten other cases with failure to reject H_0 compared to nine for the Kendall τ test.

3.3.2 Time-windowed Readout Controllers (dt Controllers)

The trend between $e_\Delta(T)$ and the normed measures of $\|s_\Delta(\xi_{\mu 0}, T)\|$ show a more complicated pattern than that of the

Table 1. Excerpt of hypothesis test results for $e(T)$ versus $\|s(\xi_{\mu 0}, T)\|$ using Kendall τ . Note the positive trend for nearest-neighbor transfers starting with $N = 7$. Also note the strong significance of the test with only the $N = 12$, $1 \rightarrow 6$ transfer failing to meet the $p < \alpha = 0.01$ threshold.

Transfer	τ for $e(T)$ vs. $\ s(\xi_{\mu 0}, T)\ $	Z_τ	p
N=3 out=1	-0.0512	-3.4191	0.0003
N=4 out=2	-0.1560	-7.2404	0.0000
N=5 out=2	-0.4969	-32.5270	0.0000
N=5 out=3	-0.2300	-13.7108	0.0000
N=6 out=2	-0.0436	-2.5253	0.0058
N=6 out=3	-0.6051	-37.9070	0.0000
N=7 out=2	0.0688	4.1724	0.0000
N=7 out=3	-0.5134	-30.9641	0.0000
N=7 out=4	-0.3464	-19.0509	0.0000
N=8 out=2	0.0723	4.0931	0.0000
N=8 out=3	-0.5216	-32.5941	0.0000
N=8 out=4	-0.2665	-9.4653	0.0000
N=9 out=2	0.0757	4.7660	0.0000
N=9 out=3	-0.4376	-27.2378	0.0000
N=9 out=4	-0.4369	-19.8395	0.0000
N=9 out=5	-0.2564	-10.5235	0.0000
N=10 out=2	0.0570	3.3822	0.0004
N=10 out=3	-0.4295	-26.5330	0.0000
N=10 out=4	-0.2229	-7.8087	0.0000
N=10 out=5	-0.2773	-8.8486	0.0000
N=11 out=2	0.0630	3.9034	0.0000
N=11 out=3	-0.4278	-26.7720	0.0000
N=11 out=4	-0.2716	-10.6654	0.0000
N=11 out=5	-0.2229	-7.6797	0.0000
N=11 out=6	-0.1746	-5.3716	0.0000
N=12 out=2	0.0878	5.3122	0.0000
N=12 out=3	-0.4619	-28.5730	0.0000
N=12 out=4	-0.2651	-9.7207	0.0000
N=12 out=5	-0.2729	-9.6384	0.0000
N=12 out=6	-0.0444	-1.1916	0.2334

t controllers, neither clearly conventional nor non-conventional. Rather, the overall trend shows a non-conventional positive correlation between $e_\Delta(T)$ and $\|s_\Delta(\xi_{\mu 0}, T)\|$ for target spins of $|\text{OUT} = 1)$ to $|\text{OUT} = 4)$ but a conventional, negative trend for transfers with $|\text{OUT} \geq 5)$. However, specifically for the tests concerning $e_\Delta(T)$ versus $\|s_\Delta(\xi_{\mu 0}, T)\|_H$ the test results in uniform refutation of H_0 in favor of H_{1-} for the localization cases where $|\text{OUT} = 1)$ and with $p < \alpha = 0.01$ for all tests. Table 2 provides a characteristic example of the Kendall τ -based hypothesis test for $e_\Delta(T)$ versus $\|s_\Delta(\xi_{\mu 0}, T)\|_H$ for $N = 3$ though $N = 12$. In summary of the Kendall τ -based hypothesis test for the time-windowed controllers we observe the following:

- Of the 108 test cases for the trend in $e_\Delta(T)$ versus $\|s_\Delta(\xi_{\mu 0}, T)\|$, 21 fail to meet the minimum confidence level and are not considered. However, for the 66 cases of

localization ($|\text{OUT} = 1)$) or transfers to $|\text{OUT} \leq 4)$, only three fail to meet the required confidence level. Of the remaining 63 tests for localization or transfer up to $|\text{OUT} = 4)$, the hypothesis test rejects H_0 in favor of H_{1+} , a non-conventional trend. In contrast, of the 42 tests for transfer to $|\text{OUT} \geq 5)$, 18 fail to meet the required confidence level. However the remaining 24 tests all display a negative, conventional trend, for these transfers.

- For the tests of $e_\Delta(T)$ versus $\|s_\Delta(\xi_{\mu 0}, T)\|_C$, we see a higher percentage of tests that fail to meet the minimum confidence level, 36 of 108. In terms of trends, all localization or nearest-neighbor transfers show a non-conventional trend for sensitivity to controller uncertainty. Of the 56 tests for transfers to $|\text{OUT} \geq 4)$, 24 fail to make the cut, but the remaining 32 test all show a conventional trend. Finally, we note that of the 16 next-nearest neighbor transfers, 14 do not show a $p < 0.01$, and the two that do, for $N = 5$ and $N = 6$ display the non-conventional behavior.
- The relation between $e_\Delta(T)$ and $\|s(\xi_{\mu 0}, T)\|_H$ shows a solid trend of conventional behavior for localization with a non-conventional trend for transfer to spins $|\text{OUT} \leq 4)$, but inconclusive results for the remaining cases. Specifically of the 18 localization tests, all show a conventional trend with high confidence. Conversely, of the 48 cases of transfer for $|\text{OUT} \leq 4)$, all display a positive, non-conventional trend with $p < 0.01$. However, the remaining 42 test cases fail to display a clear trend with the majority, 32, failing to meet the required confidence level and the remainder displaying no clear trend.

As a check on consistency, we compare the Kendall τ -based hypothesis test results with that obtained from the Pearson r . As with the case of the instant-readout controllers, we see strong agreement between the two measures, in detail:

- For $e_\Delta(T)$ versus $\|s_\Delta(\xi_{\mu 0}, T)\|$, the 66 test cases for localization through $|\text{OUT} \leq 4)$, disagree in only three cases. The Kendall τ provides inconclusive results for $N = 6$, $1 \rightarrow 3$ transfer and $N = 8$ localization, while the Pearson r results show unconventional trends for these transfers but is inconclusive on the $N = 7$, $1 \rightarrow 4$ transfer. In the remaining 63 test cases for $|\text{OUT} \leq 4)$, the tests agree on an unconventional trend. While of the remaining 42 test cases, the Pearson r results in 21 inconclusive tests versus 20 for the Kendall τ , all cases in which both tests present $p < 0.01$ agree on a conventional trend for these transfers.
- For controller uncertainty, the $e_\Delta(T)$ versus $\|s(\xi_{\mu 0}, T)\|_C$ trends show perfect agreement in rejecting H_0 in favor of H_{1+} for all localization and nearest-neighbor transfers. In terms of the next-nearest neighbor transfers (those transfers to $|\text{OUT} = 3)$, the Pearson-based test agrees with the Kendall τ -based test in rejection of H_0 in favor of H_{1+} for $N = 5$ and $N = 6$. However, for the remaining 14 next-nearest neighbor transfer, the Pearson r test statistic provides inconclusive results. For the 56 test cases for $|\text{OUT} \geq 4)$, the Pearson r -based test returns 18 instances that fall below the confidence threshold. However, in all

Table 2. Excerpt of hypothesis test results for $e_{\Delta}(T)$ versus $\|s_{\Delta}(\xi_{\mu 0}, T)\|_H$ using the Kendall τ . Of note are the conventional trends for all localization cases with $p < \alpha = 0.01$, and the unconventional, positive trend for all transfer $|2 \leq \text{OUT} \leq 5)$ with strong confidence. The trend for transfer to $(\text{OUT} \geq 5)$ is inconclusive.

Transfer	τ for $e_{\Delta}(T)$ vs. $\ s_{\Delta}(\xi_{\mu 0}, T \pm \Delta T)\ _H$	Z_{τ}	p
N=3 out=1	-0.6364	-42.5924	0.0000
N=3 out=2	0.4810	32.1507	0.0000
N=4 out=1	-0.3415	-18.9007	0.0000
N=4 out=2	0.3509	13.3935	0.0000
N=5 out=1	-0.6548	-43.7457	0.0000
N=5 out=2	0.4997	30.1915	0.0000
N=5 out=3	0.4533	27.2474	0.0000
N=6 out=1	-0.6431	-35.4519	0.0000
N=6 out=2	0.2621	12.9521	0.0000
N=6 out=3	0.3070	18.0456	0.0000
N=7 out=1	-0.6773	-45.2345	0.0000
N=7 out=2	0.3447	18.5525	0.0000
N=7 out=3	0.2993	17.4544	0.0000
N=7 out=4	0.2610	12.5108	0.0000
N=8 out=1	-0.7214	-40.1470	0.0000
N=8 out=2	0.2749	15.5228	0.0000
N=8 out=3	0.3501	20.0874	0.0000
N=8 out=4	0.1286	4.6277	0.0000
N=9 out=1	-0.7302	-48.8551	0.0000
N=9 out=2	0.3203	16.8054	0.0000
N=9 out=3	0.3454	19.9429	0.0000
N=9 out=4	0.1102	4.4269	0.0000
N=9 out=5	-0.0020	-0.0718	0.4717
N=10 out=1	-0.8023	-44.2737	0.0000
N=10 out=2	0.2107	10.3089	0.0000
N=10 out=3	0.4274	25.0752	0.0000
N=10 out=4	0.1184	4.5067	0.0000
N=10 out=5	0.0448	1.4231	0.0773
N=11 out=1	-0.7652	-51.1965	0.0000
N=11 out=2	0.2871	15.0261	0.0000
N=11 out=3	0.4060	23.6861	0.0000
N=11 out=4	0.1651	7.3577	0.0000
N=11 out=5	-0.0556	-1.6805	0.0464
N=11 out=6	0.1131	3.2609	0.0006
N=12 out=1	-0.8222	-44.9496	0.0000
N=12 out=2	0.1577	7.9024	0.0000
N=12 out=3	0.4148	23.9986	0.0000
N=12 out=4	0.1737	7.6659	0.0000
N=12 out=5	-0.0303	-0.9387	0.1739
N=12 out=6	-0.0571	-1.3528	0.0881

cases where both the Kendall τ and Pearson r present high confidence, the hypothesis test agrees in rejection of H_0 for H_{1-} for these transfers.

- Of the 108 test cases for $e_{\Delta}(T)$ versus $\|s_{\Delta}(\xi_{\mu 0}, T)\|_H$, we

see agreement between both measures in 100 cases. The 8 conflicts arise from one test or the other failing to reject the null hypothesis while the other does reject H_0 , but in no cases to both tests reject H_0 in favor of opposing alternative hypotheses. Of note, for the conventional trend of localization assessed by the Kendall τ -based test, the Pearson r test agrees on all counts save for $N = 5$ and $N = 12$, which are inconclusive based on the Pearson r .

3.4 Equivalent Error - Widely Varying Robustness

Though the hypothesis test of Section 3.3 provides insight into the trends of error versus log-sensitivity on a large scale, it does not tell the entire story. In fact, one of the more interesting features of the controllers in this data set is the range of log-sensitivity observed for a given fidelity error. Figure 1 displays the log-sensitivity for controller and Hamiltonian perturbations versus error for instant-time readout (t controllers) in a 5-ring with nearest neighbor transfer. The overall trend of the figure confirms the negative trend of the hypothesis test, but the spread of log-sensitivities for a given error is large. For example, the log-sensitivity for controllers with a fidelity error $e(T) = 10^{-5}$ ranges from as low as 10^0 to greater than 10^5 . This belies a simple one-parameter relation between log-sensitivity and error, but provides evidence for the existence of controllers with the best of possible properties: good performance and with acceptable robustness. As a second example, we show the plot of $\|s_{\Delta}(\xi_{\mu 0}, T)\|$ versus $e_{\Delta}(T)$ for a 3-ring for nearest-neighbor transfer and time-windowed readout (dt controller) in Figure 2. The plot confirms the positive (non-conventional) trend of the hypothesis test but displays wide variation in log-sensitivities in vicinity of $e(T) = 0.016$ from as low as 10^{-3} upwards to 10^5 . Identification of what factors guarantee the smaller log-sensitivities or prevent the larger values would be highly beneficial in the process of controller design and selection, but remain an open question.

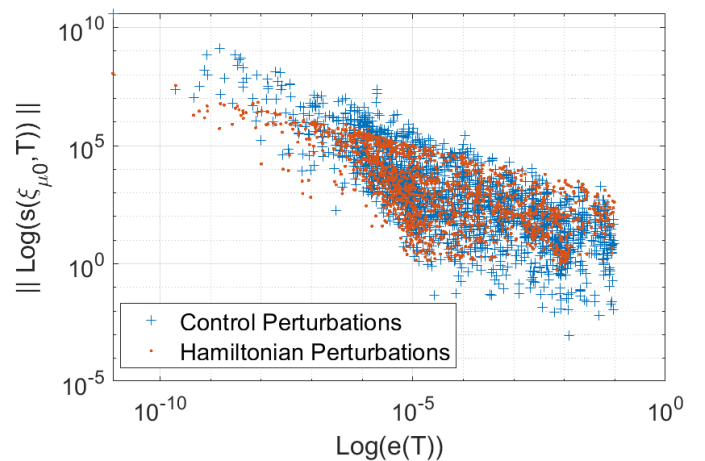


Figure 1. Log-log plot of $\|s_{\Delta}(\xi_{\mu 0}, T)\|_C$ (blue crosses) and $\|s_{\Delta}(\xi_{\mu 0}, T)\|_H$ (red dots) versus $e(t)$ for a nearest-neighbor transfer in a $N = 5$ ring. Note the overall negative (conventional) trend, but also the variation in log-sensitivity by orders of magnitude for controllers on the same vertical line.

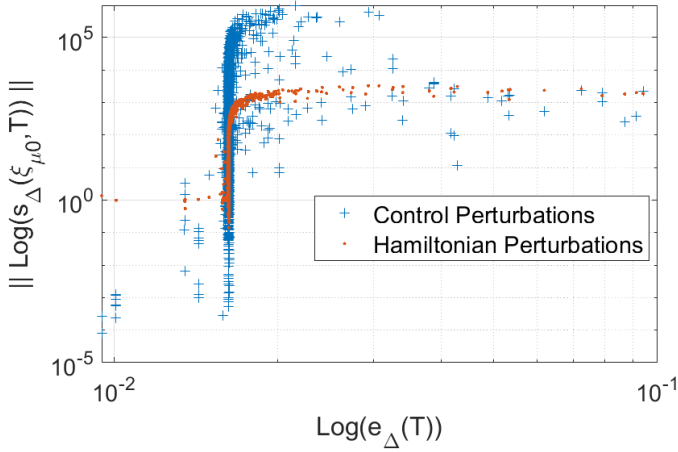


Figure 2. Log-log plot of $\|s_{\Delta}(\xi_{\mu 0}, T)\|_C$ (blue crosses) and $\|s_{\Delta}(\xi_{\mu 0}, T)\|_H$ (red dots) versus $e_{\Delta}(t)$ for a nearest-neighbor transfer in a $N = 3$ ring for time-windowed readout. Note the major variations in log-sensitivity for controllers with an error in the range of 0.016.

Next we note the visual depiction of the nearest-neighbor transfers for instantaneous read-out controllers with $N \geq 7$ in Figure 3. Though the hypothesis test results show rejection of H_0 in favor of H_{1+} for these cases, the trend is not readily apparent visually as seen in Figure 3. This can be confirmed by the relatively small values of the Kendall τ and Pearson r for these transfers. However, of greater importance are the variations in the log-sensitivity for a given error seen in the plot, again indicating the possibility of controllers that provide good robustness for acceptable performance.

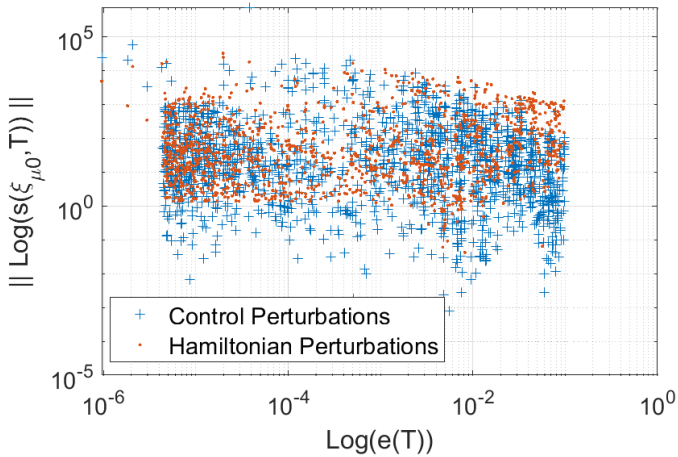


Figure 3. Log-log plot of $\|s(\xi_{\mu 0}, T)\|_C$ (blue crosses) and $\|s(\xi_{\mu 0}, T)\|_H$ (red dots) versus $e(t)$ for a nearest-neighbor transfer in a $N = 7$ and instantaneous readout. Note that a strong positive trend is not visually apparent from the plot, but the plot does display the same characteristic of widely varying log-sensitivities for the same error, suggesting the ability to select controllers with good robustness and performance.

Finally, we look at the plot of a localization transfer in Figure 4. Here we can clearly see the contrast in controller robustness for localization between Hamiltonian uncertainty

and controller uncertainty. The strong unconventional trend between $e_{\Delta}(T)$ and $\|s_{\Delta}(\xi_{\mu 0}, T)\|_C$ is clearly evident while the slightly negative conventional trend for $\|s_{\Delta}(\xi_{\mu 0}, T)\|_H$ is also perceptible. But more important is the nearly constant value of the log-sensitivity for Hamiltonian uncertainty over the range of error, a factor that can likely be exploited to provide some robustness guarantees over large performance ranges in the case of localization.

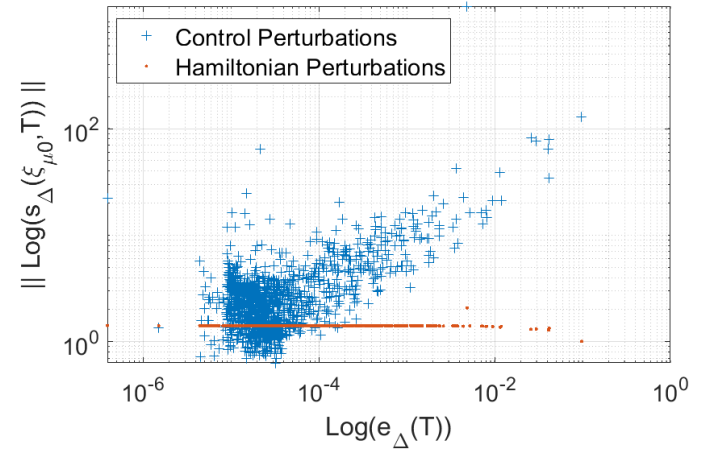


Figure 4. Log-log plot of $\|s_{\Delta}(\xi_{\mu 0}, T)\|_C$ (blue crosses) and $\|s_{\Delta}(\xi_{\mu 0}, T)\|_H$ (red dots) versus $e_{\Delta}(t)$ for $N = 6$ localization. Note the negative trend for controller uncertainty but almost flat trend for Hamiltonian uncertainty.

4. Conclusion

In this paper we have used a basic hypothesis test to determine the degree by which controllers optimized for coherent excitation transport in quantum rings abide by the limitations implied by classical control, extending the work initiated in E. Jonckheere, S. Schirmer, and F. Langbein (2018). In contrast to E. Jonckheere, S. Schirmer, and F. Langbein (2018), we extended the analysis to consider not only controllers optimized for time-averaged fidelity, but those optimized for instantaneous read-out as well. Further, we included uncertainty in both the controlling bias fields and the spin-couplings. In the main, our results confirm those of E. Jonckheere, S. Schirmer, and F. Langbein (2018) in that controllers optimized for read-out over a time window exhibit a degree of non-classical behavior for transfer to spins near the initial spin and regain conventional behavior for transfers between more distant spins. However, while the results in E. Jonckheere, S. Schirmer, and F. Langbein (2018) indicated non-conventional trends for the localization cases with Hamiltonian perturbations, using the updated calculations of (17) yields more conventional results based on the Kendall τ and Pearson r hypothesis tests. In the extension of the analysis to controllers optimized for instantaneous readout, we noted a strong conventional trend for all spin sizes and transfers, save for the nearest-neighbor transfers of $N \geq 7$. Finally, we showed that beyond just the hypothesis testing, controllers of both types display widely varying levels of robustness for the same error.

Looking to future work, we need to identify what drives the variation in log-sensitivity for controllers with similar error in order to direct synthesis towards controllers that provide the best robustness properties for a given fidelity requirement. Next, the cause for the differences in the log-sensitivity trends observed for controllers optimized for instantaneous readout vs readout over a time window, and transfer to nearest neighbor and next-nearest neighbor spins in both types of controllers needs to be elucidated to exploit those properties and potentially navigate around the limitations imposed in the context of classical control theory. Finally, it is necessary to generalize the one-uncertainty-at-a-time nature of the differential sensitivity technique used in this paper to more general methods that account for multiple structured uncertainties or even unstructured uncertainties.

Conflict of interest

The authors report no conflicts of interest.

Financial support

Sean O’Neil acknowledges PhD funding from the US Army Advanced Civil Schooling program.

Data availability

The data is available at Frank Langbein, Sean O’Neil, and Shermer (2022).

References

- Abdi, Hervé (n.d.). *The Kendall Rank Correlation Coefficient*. URL: <https://personal.utdallas.edu/~herve/Abdi-KendallCorrelation2007-pretty.pdf>.
- Chen, Chi-Tsong (2013). *Linear System Theory and Design, Fourth Edition*. New York: Oxford University Press.
- Daems, D. et al. (July 2013). “Robust Quantum Control by a Single-Shot Shaped Pulse”. In: *Physical Review Letters* 111 (5), p. 050404. ISSN: 0031-9007. DOI: 10.1103/PhysRevLett.111.050404. URL: <https://link.aps.org/doi/10.1103/PhysRevLett.111.050404>.
- Deng, Xiu-Hao, Edwin Barnes, and Sophia E Economou (July 2017). “Robustness of error-suppressing entangling gates in cavity-coupled transmon qubits”. In: *Phys. Rev. B* 96 (3), p. 35441. DOI: 10.1103/PhysRevB.96.035441. URL: <https://link.aps.org/doi/10.1103/PhysRevB.96.035441>.
- Dorf, Richard C. and Robert H. Bishop (2000). *Modern Control Systems*. 9th. USA: Prentice-Hall, Inc. ISBN: 0130306606.
- Dridi, Ghassem, Kaipeng Liu, and Stéphane Guérin (Dec. 2020). “Optimal Robust Quantum Control by Inverse Geometric Optimization”. In: *Phys. Rev. Lett.* 125 (25), p. 250403. DOI: 10.1103/PhysRevLett.125.250403. URL: <https://link.aps.org/doi/10.1103/PhysRevLett.125.250403>.
- Glaser, Steffen J. et al. (Dec. 2015). “Training Schrödinger’s cat: quantum optimal control”. In: *The European Physical Journal D* 69 (12), p. 279. ISSN: 1434-6060. DOI: 10.1140/epjd/e2015-60464-1. URL: <http://link.springer.com/10.1140/epjd/e2015-60464-1>.
- Güngördü, Utkan and J. P. Kestner (Dec. 2019). “Analytically parametrized solutions for robust quantum control using smooth pulses”. In: *Physical Review A* 100 (6), p. 062310. ISSN: 2469-9926. DOI: 10.1103/PhysRevA.100.062310. URL: <https://link.aps.org/doi/10.1103/PhysRevA.100.062310>.
- Jonckheere, E., S. Schirmer, and F. Langbein (Apr. 2018). “Jonckheere-Terpstra test for nonclassical error versus log-sensitivity relationship of quantum spin network controllers”. In: *International Journal of Robust and Nonlinear Control* 28 (6), pp. 2383–2403. ISSN: 1049-8923. DOI: 10.1002/rnc.4022. URL: <https://onlinelibrary.wiley.com/doi/10.1002/rnc.4022>.
- Kosut, Robert L, Gaurav Bhole, and Herschel Rabitz (2022). “Robust Quantum Control: Analysis and Synthesis via Averaging”. In: DOI: 10.48550/ARXIV.2208.14193. URL: <https://arxiv.org/abs/2208.14193>.
- Koswara, Andrew, Vaibhav Bhutoria, and Raj Chakrabarti (June 2021). “Quantum robust control theory for Hamiltonian and control field uncertainty”. In: *New Journal of Physics* 23 (6), p. 063046. ISSN: 1367-2630. DOI: 10.1088/1367-2630/ac0479. URL: <https://iopscience.iop.org/article/10.1088/1367-2630/ac0479>.
- Langbein, Frank, Sean O’Neil, and Sophie Shermer (2022). *Energy landscape controllers for quantum state transfer in spin-1/2 networks with ring topology*. DOI: <https://doi.org/10.33774/coe-2022-35xggg>. URL: <https://www.cambridge.org/engage/coe/article-details/63c9eda607308a0e4c9f89a9?show=item>.
- Langbein, Frank, Sophie Shermer, and Sean O’Neil (2023). *Data - Static Bias Controllers for XX Spin Rings*. URL: <https://qyber.black/spinnet/data-static-bias-controllers-xx-spin-rings>.
- O’Neil, S et al. (Dec. 2017). “Sensitivity and robustness of quantum rings to parameter uncertainty”. In: Available at arXiv:1708.09649v1, pp. 6137–6143.
- O’Neil, S. et al. (2022). *Time Domain Sensitivity of the Tracking Error*. DOI: 10.48550/ARXIV.2210.15783. URL: <https://arxiv.org/abs/2210.15783>.
- Ram, M. Harshanth et al. (Apr. 2022). “Robust quantum control using hybrid pulse engineering”. In: *Physical Review A* 105 (4), p. 042437. ISSN: 2469-9926. DOI: 10.1103/PhysRevA.105.042437. URL: <https://link.aps.org/doi/10.1103/PhysRevA.105.042437>.
- Schirmer, S. et al. (Dec. 2018). “Robustness of Energy Landscape Control for Spin Networks Under Decoherence”. In: *IEEE*, pp. 6608–6613. ISBN: 978-1-5386-1395-5. DOI: 10.1109/CDC.2018.8619179. URL: <https://ieeexplore.ieee.org/document/8619179/>.
- Schirmer, Sophie G, Edmond Jonckheere, and Frank G Langbein (Dec. 2015). “Time Optimal Information Transfer in Spintronic Networks”. In: *54th IEEE Conference on Decision and Control*, pp. 6454–6459.
- Schirmer, Sophie G., Edmond A. Jonckheere, and Frank C. Langbein (Aug. 2018). “Design of Feedback Control Laws for Information Transfer in Spintronic Networks”. In: *IEEE Transactions on Automatic Control* 63 (8), pp. 2523–2536. ISSN: 0018-9286. DOI: 10.1109/TAC.2017.2777187. URL: <https://ieeexplore.ieee.org/document/8119551/>.
- Shapira, Yotam et al. (Nov. 2018). “Robust Entanglement Gates for Trapped-Ion Qubits”. In: *Physical Review Letters* 121 (18), p. 180502. ISSN: 0031-9007. DOI: 10.1103/PhysRevLett.121.180502. URL: <https://link.aps.org/doi/10.1103/PhysRevLett.121.180502>.
- Shermer, Sophie (Sept. 2023). “What is robust control in quantum technology?” In: *Research Directions: Quantum Technologies* 1, e3. ISSN: 2752-9444. DOI: 10.1017/qut.2022.5. URL: https://www.cambridge.org/core/product/identifier/S2752944422000055/type/journal_article.
- Sontag, Eduardo D. (1998). “Feedback and Stabilization”. In: *Mathematical Control Theory: Deterministic Finite Dimensional Systems*. New York, NY: Springer New York, pp. 183–260. ISBN: 978-1-4612-0577-7. DOI: 10.1007/978-1-4612-0577-7_5. URL: https://doi.org/10.1007/978-1-4612-0577-7_5.
- Valahu, C H et al. (Oct. 2022). “Quantum control methods for robust entanglement of trapped ions”. In: *Journal of Physics B: Atomic, Molecular and Optical Physics* 55 (20), p. 204003. ISSN: 0953-4075. DOI: 10.1088/1361-6455/ac8eff. URL: <https://iopscience.iop.org/article/10.1088/1361-6455/ac8eff>.
- Weidner, Carrie Ann et al. (Dec. 2022). “Applying classical control techniques to quantum systems: entanglement versus stability margin and other limitations”. In: *61st IEEE Conference on Decision and Control*. Cancun, Mexico, pp. 5813–5818.
- Wiseman, H M and G J Milburn (2009). *Quantum Measurement and Control*. Cambridge University Press.
- Wu, Re-Bing et al. (Apr. 2019). “Learning robust and high-precision quantum controls”. In: *Physical Review A* 99 (4), p. 042327. ISSN: 2469-9926. DOI: 10.1103/PhysRevA.99.042327. URL: <https://link.aps.org/doi/10.1103/PhysRevA.99.042327>.
- Zhang, Yifan et al. (2022). *Robust quantum control for the manipulation of solid-state spins*. DOI: 10.48550/ARXIV.2205.02434. URL: <https://arxiv.org/abs/2205.02434>.
- Zhou, K. and J. C. Doyle (1998). *Essentials of Robust Control*. Prentice-Hall.